Pathological Shear Stress Stimulates the Tyrosine Phosphorylation of α-Actinin Associated with the Glycoprotein Ib-IX Complex†

Shuju Feng,‡ Julio C. Reséndiz,‡ Nicolaos Christodoulides,‡ Xin Lu,‡ David Arboleda,‡ Michael C. Berndt,§ and Michael H. Kroll*,‡

Veterans' Affairs Medical Center, Baylor College of Medicine and Rice University, Houston, Texas 77030, and Baker Medical Research Institute, Victoria, Australia

Received July 23, 2001; Revised Manuscript Received November 9, 2001

ABSTRACT: Shear-induced platelet responses are triggered by VWF binding to the platelet GpIb-IX complex, and there is evidence that this ligand−receptor coupling stimulates transmembranous signaling through the cytoplasmic tail of glycoprotein (Gp) Ibα. To investigate the mechanism by which signaling is effected, new molecular interactions involving GpIb-IX that develop in response to pathological shearing stress were examined in intact human platelets. Exposure to shear, but not α-thrombin, results in the co-immunoprecipitation of the actin cross-linking protein α-actinin with the GpIb-IX complex. Blockers of VWF binding to GpIbα or actin polymerization inhibit the association of α-actinin with the GpIb-IX complex, but the association of α-actinin with the GpIb-IX complex is not affected by inhibiting VWF binding to platelet integrin αIIbβ3 (GpIIb-IIIa). α-Actinin becomes tyrosine phosphorylated in response to pathological shear stress, and phosphorylated α-actinin associates with GpIb-IX. In resting platelets, class IA heterodimeric phosphatidylinositol 3-kinase (PI 3-K) and protein kinase N (PKN) associate with nonphosphorylated α-actinin. Shear stress causes PI 3-K to disassociate from α-actinin, while it stimulates PKN binding to α-actinin. These results demonstrate that shear-induced VWF binding to GpIbα causes enhanced binding of cytoskeletal α-actinin to GpIb-IX and suggest that α-actinin, perhaps through tyrosine phosphorylation, serves as an adapter for a signaling complex that could regulate VWF-induced platelet aggregation.

Platelet deposition at sites of vascular injury triggers pathological arterial thrombosis. The development of an occlusive arterial thrombus occurs within a rheological milieu that includes elevated wall shearing stress. Such pathological shearing stress generates frictional forces between platelets and the damaged vessel wall that induce very specific ligand−receptor interactions required for platelet adhesion, activation, and aggregation. The initial attachment of platelets to freshly exposed subendothelium involves the platelet glycoprotein (Gp)[1] Ib-IX complex binding to von Willebrand factor (VWF), with stable attachment facilitated by collagen binding to platelet α2β1, and thrombus formation established by shear-induced VWF binding to the activated αIIbβ3 complex (*1*−*5*). The VWF−GpIb-IX interaction initiates thrombus formation by signaling platelet secretory pathways and the activation of αIIbβ3 (*6*−*10*). These two responses amplify the triggering stimulus by increasing local concentrations of proaggregatory and vasoconstricting agonists, and by effecting the forces of platelet cohesion capable of withstanding shearing stresses that sweep away leukocytes and locally generated fibrin polymers (*11*−*13*).

Mechanisms of GpIb-IX signaling are poorly understood. Our laboratory has examined the hypothesis that signaling by GpIb-IX is mediated by molecular interactions involving the carboxyl-terminal cytoplasmic tail of GpIbα. The rationale for this hypothesis is based on several observations. The first is that most platelet signaling under pathological shearing stress depends on VWF binding to the extracellular domain of GpIbα (*6*−*10*). The second observation is that the cytoplasmic domain of GpIbα is the longest carboxyl-terminal tail of all of the VWF receptor complex components (96 amino acids, vs 36 for GpIbβ and 6 for GpIX) and that it is highly conserved among humans, dogs, and mice (*14*, *15*). The third fact supporting the idea that the cytoplasmic domain of GpIbα is a good candidate signal transducer is that it binds directly to the membrane skeleton through filamin A (*16*, *17*) and that it binds directly to a 14-3-3ζ adapter protein (*18*). Both of these connections, in many cell types (including platelets), are implicated in signal transduction in response to either mechanical forces or soluble ligands. Finally, and perhaps most compellingly, the full-length cytoplasmic domain of recombinant GpIbα is required for signal transduction in two different heterologous cell systems (*19*, *20*).

α-Actinin is a protein that cross-links actin polymers. It is involved in organizing the membrane (or cortical) skeleton intimately interdigitated, through filamin A connections, with

† This work was supported in part by the American Heart Association, Department of Veterans' Affairs Research Service, the National Institutes of Health (Grants HL18454 and HL65967), and the National Heart Foundation of Australia.

* To whom correspondence should be addressed: Section of Hematology-Oncology (111H), VA Medical Center, 2002 Holcombe Blvd., Houston, TX 77030. Telephone: (713) 794-7111. Fax: (713) 794-7733. E-mail: mkroll@bcm.tmc.edu.

‡ Baylor College of Medicine and Rice University.

§ Baker Medical Research Institute.

[1] Abbreviations: Gp, glycoprotein; mAb, monoclonal antibody; PI 3-K, phosphatidylinositol 3-kinase; PKN, protein kinase N; VWF, von Willebrand factor.

10.1021/bi0156005 CCC: $22.00
Published on Web 01/04/2002

the cytoplasmic tail of at least 25 000 transmembranous GpIbα molecules on the resting discoid platelet surface. Following platelet activation, α-actinin undergoes rapid disassociation and reassociation reactions with actin that mediate dynamic structural changes leading to platelet spreading, lamellipodia and filopodia generation, granule secretion, and receptor up- and downregulation. There is recent evidence that α-actinin within the matrix of the actin scaffold regulates enzymatic reactions by binding to phosphoinositides, including phosphatidylinositol 4,5-bisphosphate (PIP_2) and phosphatidylinositol 3,4,5-trisphosphate (PIP_3) (*21*, *22*). In this capacity, α-actinin regulates phospholipid substrate availability, localizes phospholipid binding proteins, and modulates phospholipid cofactor regulation of several important signaling enzymes, including class 1A (heterodimeric) phosphatidylinositol 3-kinase (PI 3-K) and protein kinase N (*21*, *22*). α-Actinin-mediated colocalization of an enzyme and its phospholipid substrate or cofactor may be modulated by its tyrosine phosphorylation (*23*, *24*).

In considering α-actinin's connection to the cytoplasmic tail of GpIbα through the platelet cytoskeleton, and in recognition of its potential functional versatility, we developed the hypothesis that α-actinin localizes signaling molecules involved in transducing GpIbα-mediated stimulatory responses initiated by shear-induced VWF binding. To investigate this hypothesis, we examined GpIbα−α-actinin interactions in intact human platelets subjected to pathological shearing stress in a cone−plate viscometer.

EXPERIMENTAL PROCEDURES

Materials. BM-75.2, a monoclonal mouse IgM anti-α-actinin antibody, and polyclonal rabbit anti-α-actinin IgG were from Sigma (St. Louis, MO). AN51, a monoclonal mouse IgG_{2a} anti-human platelet GpIbα antibody that recognizes its ligand-binding domain, was from DAKO (Carpinteria, CA). WM23, a mouse monoclonal antibody that recognizes the macroglycopeptide domain of GpIbα, was from the Baker Medical Research Institute. AK2, a mouse monoclonal IgG_1 anti-human GpIbα antibody, was purchased from RDI Inc. (Flanders, NJ). B-9, a monoclonal mouse IgG_1 anti-PI 3-K p85 subunit antibody, I-19, a goat polyclonal anti-actin antibody, and integrin β3, a goat polyclonal anti-β3 antibody, were from Santa Cruz Biotechnology, Inc. (Santa Cruz, CA). 4G10, a monoclonal mouse IgG_{2bk} anti-phosphotyrosine antibody, a rabbit polyclonal antibody to PKN, and a rabbit IgG anti-PI 3-K p85 antibody were from Upstate Biotechnology (Lake Placid, NY). Rabbit polyclonal anti-β3 antiserum was generously provided by P. Thiagarajan (Baylor College of Medicine). ECL reagents, protein A−Sepharose beads, autoradiography film, and rainbow molecular mass standards were purchased from Amersham Life Science Inc. (Arlington Heights, IL). Purified human VWF was from Calbiochem (La Jolla, CA). Human thrombin, leupeptin, aprotinin, phenylmethanesulfonyl fluoride (PMSF), pepstatin A, EDTA, bovine serum albumin, ristocetin, anti-goat IgG peroxidase-conjugated antibody, dimethyl sulfoxide (DMSO), the synthetic Arg-Gly-Asp-Ser peptide (RGDS), and other miscellaneous chemical reagents were purchased from Sigma. Piceatannol was purchased from Boehringer Mannheim (Indianapolis, IN).

Preparation of Washed Platelets. Venous blood was obtained from healthy volunteer donors and collected in a 15% (v/v) acid/citrate/dextrose mixture (ACD). Blood was centrifuged at 270*g* for 14 min at 24 °C, and the platelet rich plasma was acidified to pH 6.5 with ACD and treated with 5 mM phosphocreatine (CP) and 25 units/mL creatine phosphokinase (CPK). The platelets were then separated from the platelet rich plasma by a second centrifugation at 1600*g* for 15 min at 24 °C. The platelets were washed in Tyrode's buffer [138 mM sodium chloride, 2.9 mM potassium chloride, 12 mM sodium bicarbonate, 0.36 mM sodium phosphate, and 5.5 mM glucose (pH 6.5)] containing CP and CPK. Washed platelets were centrifuged at 1200*g* for 10 min at 24 °C. The pellet was then resuspended in JNL buffer (6 mM glucose, 130 mM NaCl, 9 mM $NaHCO_3$, 10 mM sodium citrate, 10 mM Tris base, 3 mM KCl, 2 mM Hepes, and 0.9 mM $MgCl_2$ with 1 mM $CaCl_2$ at pH 7.35) at a concentration of 2.5×10^8 platelets/mL. The amount of VWF remaining in the platelet suspension following this washing procedure was measured three times using a micro-latex immunoassay (Diagnostica Stago, Parsippany, NJ): 4, 9, and 3%. In experiments where inhibition of VWF binding to platelets was desired, the mAb AK2 was added to the washed platelet suspensions at a final concentration of 6 μg/mL, or the RGDS peptide was added at a final concentration of 0.5 mM, for 15 min prior to exposure to shear.

Shear Stress System. Washed human platelets were subjected to fluid shear stress in a cone−plate viscometer at 24 and 37 °C (*3*). Immediately after shear, samples were lysed in ice-cold immunoprecipitation buffer containing (final concentrations) 1% Triton X-100, 1 mM Na_3VO_4, 1 mM NaF, 1 mM EGTA, 0.1 mM PMSF, and aprotinin, pepstatin, and leupeptin (5 μg/mL each). For platelet aggregation measurements, 5 μL of control or sheared platelet samples was dispersed in 10 mL of Isoton II (Coulter Electronics, Inc., Hialeah, FL) diluent containing 0.25% glutaraldehyde (final concentration). The particle size distribution and counts were determined with an electronic particle counter (model ZB1 with Channelyzer, Coulter Electronics, Inc.) using a sample volume of 100 μL and a 50 μm diameter aperture. Particles that were within ±20% of the mean platelet size in the control, unsheared samples were considered single platelets. The percent decrease in the number of single platelets was a measure of platelet aggregation. In some experiments, platelet aggregation was assessed by flow cytometry. A sample (5 μL) was fixed in a 0.5 mL solution of 2% paraformaldehyde, and single platelets were identified in a resting (time zero) suspension by their forward scatter-side scatter properties, with a decrease in the signal of this gate in sheared samples representing a decrease in the number of single platelets. Stirred washed platelets were also stimulated with α-thrombin (1 unit/mL) or purified VWF (5 μg/mL) with ristocetin (1.0 mg/mL). Their aggregation was monitored nephelometrically at 37 °C in an aggregometer (Chronolog), and samples were collected for analyses as described below.

Immunoprecipitation and Western Blotting Analysis. Sheared platelet or control samples were lysed as described above. Samples were then sonicated briefly (~5 s) and incubated on ice for 30 min. Platelet lysates were cleared of insoluble debris by centrifugation at 13000*g* for 15 min at 4 °C, and then diluted with the same volume of ice-cold phosphate-buffered saline (PBS) to bring the final Triton X-100 concentration to 0.5%. GpIbα was immunoprecipitated using

either the mAb AN51 or WM23. αIIbβ3 was immunoprecipitated with the rabbit anti-β3 polyclonal antibody. The p85 subunit of PI 3-K was immunoprecipitated with the mouse monoclonal (B9) or rabbit polyclonal antibody, and PKN was immunoprecipitated using a rabbit polyclonal antibody. The α-actinin was immunoprecipitated with the mouse monoclonal IgM antibody BM 75.2. Immunoprecipitation was carried out by incubating platelet lysates with an antibody overnight at 4 °C followed by a 1 h incubation at 4 °C with 40 μL of Sepharose-conjugated protein A (or 30 μL of agarose-conjugated protein A/G for the I-19 immunoprecipitations or 40 μL of agarose-conjugated anti-mouse IgM for α-actinin). Following three washes with ice-cold PBS, precipitated proteins were separated by SDS−polyacrylamide gel electrophoresis (PAGE) under reducing conditions and transferred onto polyvinylidene difluoride (PVDF) or nitrocellulose membranes (Bio-Rad). Proteins were then visualized using either silver staining, Coomassie blue staining, or Western blotting. The Western blotting procedure was carried out using primary antibodies overnight at 4 °C, followed by incubation for 1 h at room temperature with the appropriate peroxidase-conjugated secondary antibodies. Reactive bands were visualized by chemiluminescence and autoradiography.

Densitometry and Quantitation of α*-Actinin Binding to GpIb-IX.* To calculate the level of α-actinin binding to GpIbα, densitometry was used to measure the amount of α-actinin co-immunoprecipitating with GpIbα. To measure the amount of GpIb-IX-associated α-actinin relative to the total amount of platelet α-actinin, immunodetectable α-actinin was measured densitometrically in serial dilutions of Triton X-100-lysed platelets fractionated into a low-speed supernatant (membrane or cortical skeleton with the soluble fraction) and a low-speed pellet (cytoskeleton). The relative transmission densitometry of these serially diluted fractions was combined and then compared to the densitometry of α-actinin in immunoprecipitates of GpIb-IX. Densitometry measurements were taken using a LKB Bromma Ultra Scan XL Enhanced Laser Densitometer (Pharmacia).

Sequence Determination. Lysates of shear stress-activated platelets were immunoprecipitated with AN51. Immunoprecipitated proteins were separated by 6% SDS−PAGE, transferred to PVDF membranes, stained with 0.05% Coomassie blue in 5% acetic acid and 10% methanol for 30 min, and destained with 5% acetic acid and 10% methanol until the bands were easily distinguished from background. The membrane was rinsed with water for 15 min, and bands of interest were excised, placed in individual microfuge tubes, and subjected to proteolytic digestion with trypsin and/or endoprotease Asp-N. The proteolytically generated fragments were derivatized with diphenylhydantoin, separated by high-performance liquid chromatography, and analyzed using a PROCISE-cLC automated sequencer.

Statistical Analyses. Densitometry data were compared using Sigma Plot to calculate means, standard error of means, and *P* values (by the Student's *t* test).

RESULTS

To begin to explore mechanisms of shear stress-induced signal transduction by the cytoplasmic tail of GpIbα, we first examined immunoprecipitates of GpIbα from washed human platelets aggregating in response to a shear stress of 120 dyn/cm^2 generated by a cone−plate viscometer. This shear stress is considered "pathological" because it is elevated beyond that observed under conditions of physiological arterial blood flow in vivo (*3*). Figure 1A shows platelet aggregation when washed platelets are treated with 1 unit/mL α-thrombin (T) or shear, and the influence of temperature on shear-induced platelet aggregation. Figure 1A also shows that shear-induced aggregation is inhibited by pretreating platelets with the mAb AK2, which binds to the ligand recognition domain of GpIbα and inhibits VWF binding. Figure 1B is a silver stain of proteins co-immunoprecipitated with GpIbα from lysates of platelet sheared for 2 min at 120 dyn/cm^2. It shows that there is a band at a molecular mass of ~100000 Da developing in sheared platelets but not present in resting platelets (time zero) or platelets stimulated by α-thrombin for 1 min (T). At 60 and 120 s after shear, the band appears to form a doublet. Please note that coprecipitating GpIbβ and GpIX are always observed in silver stains of platelet lysates immunoprecipitated with an anti-GpIbα monoclonal antibody (data not shown).

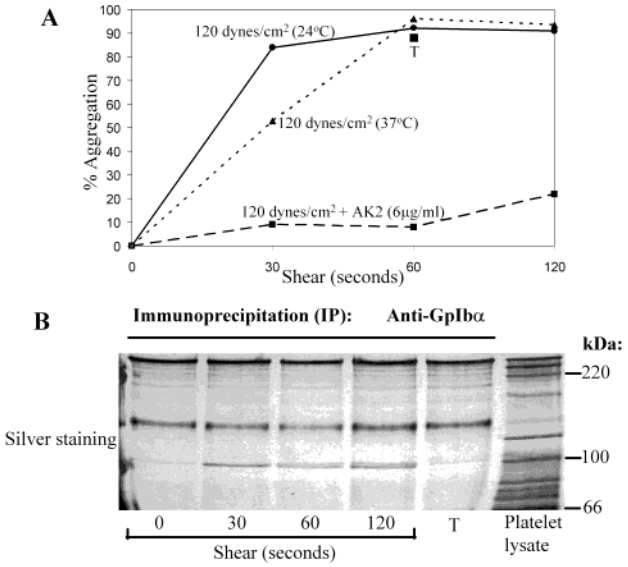

FIGURE 1: Shear stress causes platelet aggregation associated with the time-dependent co-immunoprecipitation of GpIb-IX with a 100 kDa protein. Washed human platelets (2.5×10^8/mL) were sheared in a cone−plate viscometer, at 24 or 37 °C, at a shear stress of 120 dyn/cm^2 for 0, 30, 60, and 120 s or stimulated with α-thrombin (1 unit/mL) for 60 s at 37 °C in a stirring aggregometer. Samples were processed as described in Experimental Procedures. (A) Platelet aggregation in response to a shear stress of 120 dyn/cm^2 at 24 or 37 °C and how it is affected by inhibiting VWF binding to GpIbα with the mAb AK2. (B) Silver-stained SDS−PAGE gel of sheared platelet lysates immunoprecipitated with the mAb WM23. α-Thrombin (1 U/mL) was present in lane T. Washed platelets were lysed in sample buffer, and 5 μg of total lysate protein was loaded; the results are representative of three separate experiments.

To establish the identity of the ~100 kDa protein that co-immunoprecipitates with GpIb-IX in platelets stimulated by pathological shear, the Coomassie-stained ~100 kDa band developing after 60 s of shearing was subjected to proteolytic digestion and microsequencing. Two fragments that provided sequence are identified by the double underline in Figure 2A. Data bank analysis revealed that the sequences are derived from α-actinin. Figure 2B confirms by immunoblotting (with a mouse anti-human α-actinin antibody) that

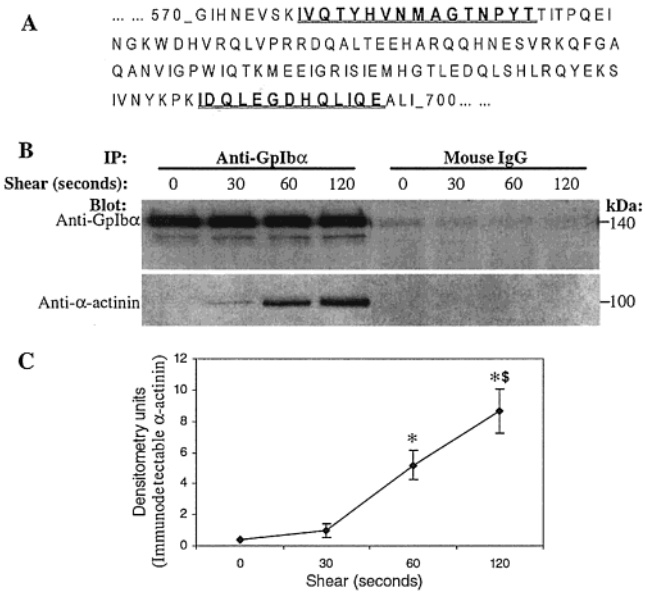

FIGURE 2: α-Actinin is the 100 kDa protein co-immunoprecipitating with GpIbα from sheared platelets. Platelets were stimulated by a shear stress of 120 dyn/cm^2 for 60 s. Samples were lysed, immunoprecipitated with the anti-GpIbα antibody WM23, and separated by 6% SDS−PAGE. The protein was then electrotransferred to a PVDF membrane and stained with Coomassie blue. The 100 kDa protein band was cut out of the membrane and digested with trypsin. Microsequencing of tryptic fragments of the 100 kDa protein band was carried out with a PROCISE-cLC sequencer. The amino acid sequence shown in Figure 2A is from the cloned human α-actinin cDNA (GenBank entry M74143). The underlined residues are those derived by microsequencing ($n = 2$). Panel B confirms by immunoblotting that shear stress leads to an increased amount of α-actinin associated with immunoprecipitated GpIbα (representative of five experiments). Panel C quantitates the time course of α-actinin's binding to GpIb-IX during 2 min of continuous shearing (mean ± SEM; one asterisk indicates that $p < 0.001$ compared with time zero; a dollar sign indicates that $p < 0.001$ compared with 60 s; $n = 3$).

α-actinin at an increased level specifically associates with GpIbα immunoprecipitated from sheared platelet lysates. To quantify the amount of shear-induced binding of α-actinin to GpIbα, densitometry of α-actinin reported by Western blotting was used to measure the amount α-actinin co-immunoprecipitated with GpIbα. Figure 2C shows that significant amounts of α-actinin associate with GpIb-IX in platelets aggregating 60 and 120 s after exposure to a shear stress of 120 dyn/cm^2.

To estimate the relative quantity of α-actinin that associates with GpIb-IX, densitometry analyses of α-actinin co-immunoprecipitating with GpIb-IX were compared to densitometric measurements of whole platelet α-actinin. Using this method, we calculated that 17.1 ± 6.1% [mean ± standard error of the mean (SEM)] of the total α-actinin associates with GpIb-IX in resting washed platelets. Two minutes after shearing at 120 dyn/cm^2, 55.6 ± 8.4% of the α-actinin binds to GpIb-IX ($n = 3$; $P < 0.001$ by the Student's *t* test). These results prove that pathological shear stress-induced platelet aggregation is associated with enhanced binding between α-actinin and GpIb-IX.

An important consideration in establishing the specificity of a platelet response to shear stress is the "dose response"; in other words, is the response a function of the magnitude of the shear stress? Figure 3A shows that the amount of immunodetectable α-actinin that co-immunoprecipitates with

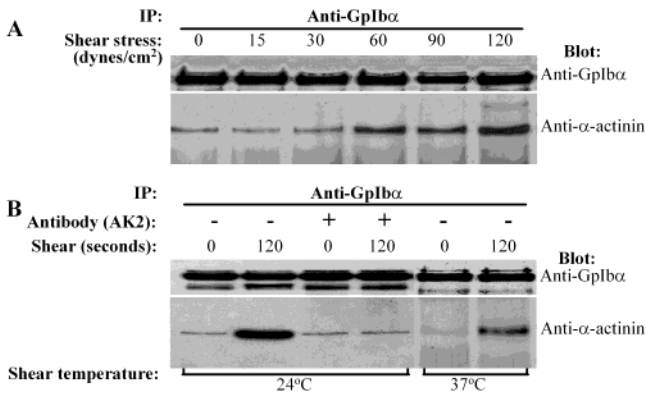

FIGURE 3: Association between α-actinin and GpIb-IX is shear-dependent, inhibited by blocking VWF binding to GpIbα, and temperature-independent. Washed platelets were sheared at varying levels of shear stress for 2 min at 24 °C (A) or at 120 dyn/cm^2 for 2 min at 24 or 37 °C (B). GpIb-IX was immunoprecipitated and the presence of immunodetectable α-actinin reported by Western blotting. In panel B, the anti-GpIbα blocking antibody AK2 (or an irrelevant mouse IgG) was preincubated with platelets at a final concentration of 6 μg/mL for 15 min (results representative of three separate experiments).

GpIb-IX after 2 min of continual shearing increases with increasing shear stress, with a threshold somewhere between 30 and 60 dyn/cm^2. Such threshold shear stresses approximate those encountered in diseased midsized human arteries, such as coronary arteries affected by atherosclerosis (*3*). These results are similar to those that we have previously reported for shear-induced protein phosphorylation and calcium responses (*7*−*9*).

To examine the receptor specificity of the enhanced interaction between GpIb-IX and α-actinin in platelets subjected to pathological shear stress, we examined how the association is affected by an inhibitor of shear-induced binding of VWF to GpIbα. Figure 3B shows that the monoclonal antibody AK2, which blocks shear-induced platelet aggregation (Figure 1), inhibits the shear-induced association of α-actinin with GpIbα. To confirm that VWF binding to GpIbα causes an increased amount of immunodetectable α-actinin in immunoprecipitates of GpIbα, washed platelets being stirred at 37 °C in a Chronolog aggregometer were analyzed after treatment with 5 μg/mL purified human VWF and 1 mg/mL ristocetin. Ristocetin-induced VWF binding to GpIbα caused increasing amounts of immunodetectable α-actinin to co-immunoprecipitate with GpIb-IX ($n = 2$; data not shown).

Another factor that could potentially result in a nonspecific interaction between α-actinin and GpIb-IX is the temperature at which the experiments were carried out (24 °C). This is because platelet cooling below physiological temperatures induces actin uncapping followed by cytoskeletal responses similar to those following stimulation by chemical agonists (*25*). The ristocetin experiments described above were carried out at 37 °C, suggesting that the association between α-actinin and GpIb-IX is not due to the experiment temperature. Nonetheless, to prove that the shear-induced interaction between α-actinin and GpIb-IX is not influenced by the temperature, experiments were carried out with the platelets and viscometer kept at 37 °C. The right side of Figure 3B shows that α-actinin co-immunoprecipitates with GpIb-IX when platelets at 37 °C are sheared for 2 min at a shear stress of 120 dyn/cm^2. The relative quantity of α-actinin that

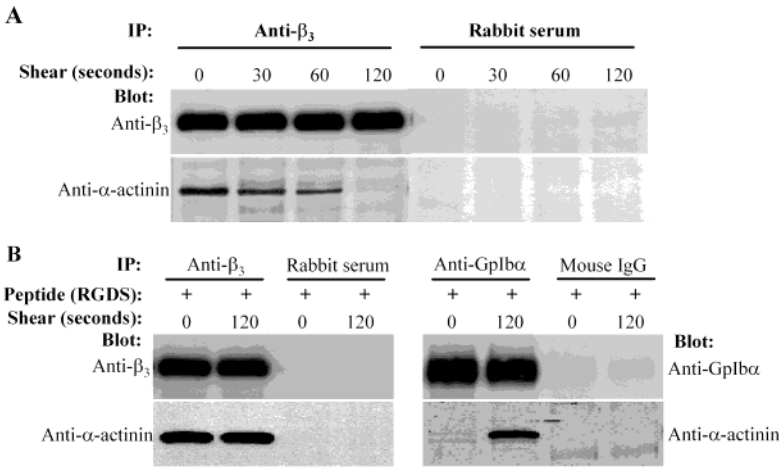

FIGURE 4: Pathological shear stress causes α-actinin to disassociate from αIIbβ3, and αIIbβ3 blockade prevents this without affecting α-actinin binding to GpIb-IX. Washed platelets were preincubated with a synthetic Arg-Gly-Asp-Ser peptide (RGDS, 0.5 mM). Platelets were then sheared, lysed, immunoprecipitated, and separated by SDS−PAGE. (A) Anti-β3 (or control antiserum)-immunoprecipitated platelets were immunoblotted for the β3 integrin and α-actinin. (B) RGDS-treated platelet lysates were immunoprecipitated with either the rabbit polyclonal anti-β3 antibody (or control serum) or the mouse anti-GpIbα antibody WM23 (or control IgG). Samples were transferred to nitrocellulose membranes and analyzed by immunoblotting followed by enhanced chemiluminescence detection (results representative of three separate experiments).

co-immunoprecipitates with GpIb-IX at 37 °C is comparable to that observed at 24 °C, indicating that shear-induced α-actinin−GpIb-IX interactions are not an artifact of temperature.

A final consideration in establishing the specificity of the shear-induced α-actinin−GpIb-IX response is to confirm that α-actinin binding to GpIb-IX is not a nonspecific consequence of the two proteins being trapped together in the "activated cytoskeleton" of sheared platelets. To do this, we examined the association of α-actinin with another surface receptor, αIIbβ3. αIIbβ3, like GpIb-IX, becomes incorporated into the activated cytoskeleton of platelets (*26*). Figure 4A shows that pathological shear stress does not cause α-actinin to associate with αIIbβ3. This indicates that the association between α-actinin and GpIb-IX, or α-actinin and αIIbβ3, does not occur simply because the molecules are separately incorporated into the cytoskeleton of platelets activated by pathological shear stress. In fact, Figure 4A shows that pathological shear stress causes α-actinin to dissociate rapidly from the β3 component of αIIbβ3, suggesting that shear also regulates the interaction between α-actinin and αIIbβ3.

Results so far indicate that platelet aggregation in response to shear stress causes α-actinin to associate with GpIb-IX, and that this response is triggered by VWF binding to GpIbα. VWF also binds to shear-activated αIIbβ3, however, and therefore, it is also possible that shear-induced VWF−αIIbβ3 interactions could signal cytoskeletal reorganization that results in α-actinin binding to GpIb-IX. To test for this possibility, washed platelets were incubated with a synthetic peptide consisting of the Arg-Gly-Asp-Ser sequence (RGDS, 0.5 mM), which blocks VWF binding to shear-activated αIIbβ3 and inhibits platelet aggregation in response to a shear stress of 120 dyn/cm^2 (*7*). Figure 4B shows that the RGDS peptide has no effect on the shear-induced association between α-actinin and GpIbα, while it inhibits the shear-induced dissociation of α-actinin from αIIbβ3. These results suggest that α-actinin's interactions with GpIb-IX are stimulated by VWF binding to GpIbα but not αIIbβ3, while the dissociation of α-actinin from αIIbβ3 is stimulated by VWF binding to the activated αIIbβ3 complex.

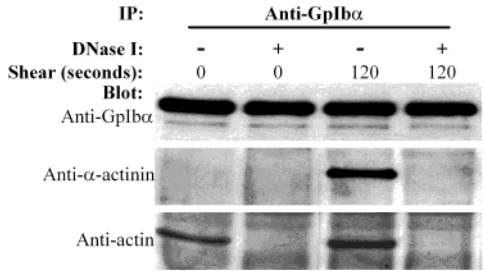

FIGURE 5: DNase I blocks the interaction between α-actinin and GpIb-IX. Sheared platelets were lysed in an equal volume of 2% Triton X-100 lysis buffer in the presence of DNase I (1 mg/mL final concentration) or 2% Triton X-100 lysis buffer with PBS (as a solvent control). Samples were analyzed by immunoprecipitating GpIbα, separating coprecipitating proteins by SDS−PAGE, and immunoblotting the separated proteins with antibodies specific for GpIbα (WM23, top panel), α-actinin (BM 75.2, middle panel), and actin (C-19, bottom panel) (results representative of three separate experiments).

Everything currently known about α-actinin and the cytoplasmic domains of GpIbα, GpIbβ, and GpIX indicates that α-actinin would bind *indirectly* to GpIb-IX by binding to GpIbα through the filamin A-actin connection. To determine if α-actinin's association with GpIbα depends on the interaction of GpIbα with the actin-based cytoskeleton, sheared platelet lysates were treated with DNase I before their incubation with the GpIbα immunoprecipitating antibody. DNase I depolymerizes actin and disrupts GpIbα−filamin A binding to the actin network. Figure 5 shows that DNase I eliminates both actin and α-actinin from GpIbα immunoprecipitates of sheared platelet lysates. This confirms that α-actinin associates with GpIb-IX through the cytoskeletal connections made by the cytoplasmic domain of GpIbα.

There is evidence that α-actinin becomes tyrosine phosphorylated when human platelets are stimulated (*23*, *24*). To determine if α-actinin is tyrosine phosphorylated in sheared platelets, we tested for the presence of tyrosine-phosphory-

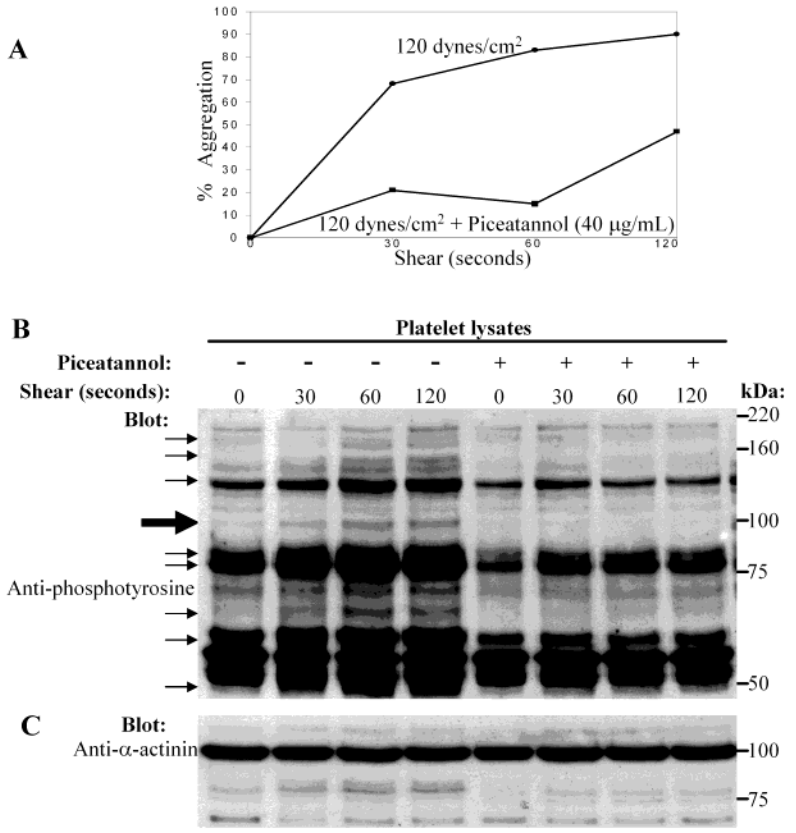

FIGURE 6: Shear stress induces the piceatannol-inhibitable tyrosine phosphorylation of multiple protein substrates, including a 100 kDa protein. Platelets were incubated with piceatannol (40 μg/mL) or dimethyl sulfoxide (as a vehicle) for 10 min before shear was started. (A) Platelet aggregation. (B) Anti-phosphotyrosine antibody (4G10) immunoblots. Small arrows denote tyrosine-phosphorylated proteins with molecular masses of 180, 150, 120, 80, 76, 65, 60, and 50 kDa. The big arrow points to a 100 kDa tyrosine-phosphorylated protein. The left four lanes contained control platelets, and the right four lanes contained piceatannol-treated platelets. Panel C shows the same membrane stripped and reprobed with an anti-α-actinin antibody (results representative of three separate experiments).

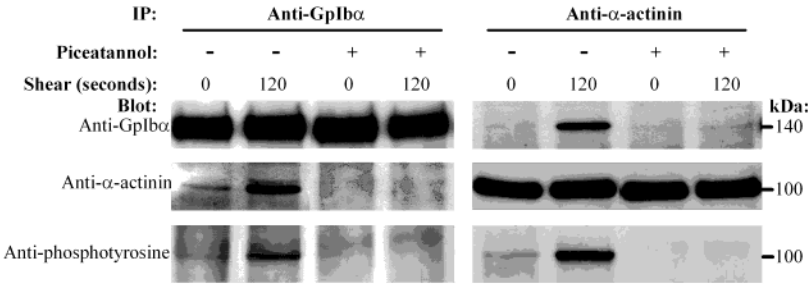

FIGURE 7: Shear-induced tyrosine phosphorylation of α-actinin regulates its binding to GpIb-IX. Washed platelets were incubated with 40 μg/mL piceatannol or an equal volume of dimethyl sulfoxide for 10 min before shear. Sheared samples were lysed, immunoprecipitated with an anti-GpIbα or anti-α-actinin antibody, and separated by SDS−PAGE. Proteins were then transferred to a nitrocellulose membrane and immunoblotted with the anti-GpIbα antibody WM23 (top panel), the rabbit polyclonal anti-α-actinin antibody (middle panel), and the anti-phosphotyrosine antibody 4G10 (bottom panel) (results representative of three separate experiments).

lated α-actinin in whole platelet lysates by immunoblotting them with phosphotyrosine-specific antibody 4G10. Figure 6B shows that many proteins are tyrosine phosphorylated in response to a shear stress of 120 dyn/cm^2, including an ~100 kDa protein identified by the large arrow on the left. Similar results have been previously reported (*9*, *10*). The right side of Figure 6B shows that piceatannol, which inhibits focal adhesion kinase, Syk, and *src* family tyrosine kinases (*27*), greatly attenuates shear-induced tyrosine phosphorylation of many different protein substrates. Piceatannol also partially inhibits shear-induced platelet aggregation (Figure 6A). Figure 6C presents the blot in Figure 6B after it was stripped and reprobed with an antibody to α-actinin. This shows that the electrophoretic mobility of α-actinin is identical to that of the tyrosine-phosphorylated protein band represented by the large arrow in Figure 6B.

To prove that the ~100 kDa tyrosine-phosphorylated band in Figure 6 is α-actinin, proteins co-immunoprecipitated with GpIbα were subjected to immunoblotting with the phosphotyrosine-specific antibody, and proteins precipitated with an antibody to α-actinin were subjected to immunoblotting with both phosphotyrosine- and GpIbα-specific antibodies. Figure 7 shows that a shear stress of 120 dyn/cm^2 causes the tyrosine phosphorylation of α-actinin that is associated with GpIbα. Figure 7 also shows that piceatannol inhibits the co-immunoprecipitation of α-actinin with GpIb-IX, suggesting that a tyrosine kinase regulates the association between α-actinin and GpIb-IX.

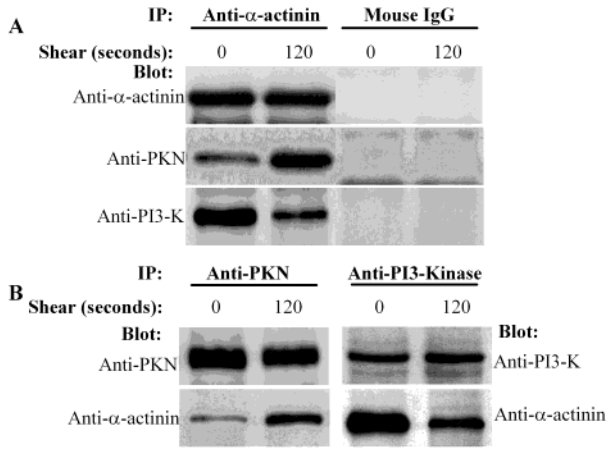

FIGURE 8: α-Actinin is an adapter protein that binds to phosphatidylinositol 3-kinase (PI 3-K) in resting platelets and protein kinase N (PKN) in sheared platelets. Panel A shows that 120 s of 120 dyn/cm^2 shear stress causes PI 3-K to dissociate from immunoprecipitated α-actinin and PKN to associate with immunoprecipitated α-actinin. Panel B confirms these results using reciprocal immunoprecipitations (results representative of three separate experiments).

The association between α-actinin and GpIb-IX juxtaposes a molecule that binds phospholipids and is tyrosine phosphorylated (α-actinin) with a molecule that demonstrates the unique property of shear-induced ligand recognition and signaling (GpIbα). Such juxtaposition raises the possibility that α-actinin could serve as an adapter protein regulating the assembly of a signaling complex involved in shear-induced platelet aggregation. To explore this hypothesis, we examined immunoprecipitates of α-actinin from sheared platelet lysates for the presence of signaling proteins that are known to associate with α-actinin. Figure 8A shows that after platelets are subjected to a shear stress of 120 dyn/cm^2 for 2 min, protein kinase N (PKN) associates further with α-actinin, while class 1A (heterodimeric) phosphatidylinositol 3-kinase (PI 3-K) disassociates from α-actinin. Figure 8B confirms these results using reciprocal immunoprecipitations. These results suggest that α-actinin serves as an adapter protein during the assembly of enzyme complexes that could contribute to shear-induced platelet aggregation.

DISCUSSION

Platelets are stimulated when ristocetin induces VWF binding to the GpIb-IX complex (*28*, *29*). Ristocetin is not, however, a physiological modulator of VWF binding. The only physiological (and pathophysiological) modulator of VWF binding to GpIb-IX identified at this time is shear stress, which is a frictional force generated by the laminar flow of blood through the vascular circuit (*3*−*5*). It is therefore useful to examine mechanisms of VWF-induced platelet activation in experimental systems capable of generating constant and uniform shearing stress. We chose to use a cone−plate viscometer because it immediately generates the target shearing stress throughout the entire platelet suspension ("bulk phase"), and because it accommodates sample volumes appropriate for biochemical analyses (*7*−*9*).

When washed platelets are sheared at a shear stress of 120 dyn/cm^2, they aggregate because VWF binds to the extracellular domain of GpIbα. VWF binding to GpIbα causes platelet cohesion, and it also causes platelet activation resulting in secretion and additional platelet cohesion through VWF binding to activated αIIbβ3 (*7*−*12*). Several potential stimulatory responses have been described, including an elevated level of cytosolic ionized calcium and the activation of protein and lipid kinases (*7*−*10*, *29*, *30*). The mechanism by which VWF binding is coupled to these platelet responses is not known, although there is evidence from heterologous cell systems that the cytoplasmic tail of recombinant GpIbα transduces signals originating when VWF binds to the extracellular region of GpIbα (*19*, *20*).

α-Actinin is a ubiquitous and potentially versatile molecule. It provides structural support by binding to cytoskeletal proteins. It regulates cellular responses by binding to adhesion receptors, signaling proteins, and inositol-containing phospholipids. It is a substrate for tyrosine kinases, and its tyrosine phosphorylation may couple nonreceptor tyrosine kinases to cytoskeletal responses. Because there is shear-induced tightening of the connections between GpIb-IX and the cytoskeleton (*31*) that might localize α-actinin to a GpIbα-based compartment, and because there is evidence that GpIbα's interactions with the cytoskeleton could regulate shear-induced signaling (*15*), we looked for changes in the molecular associations between α-actinin and GpIbα induced by pathological shear stress. We observed that shear stress causes an increased level of binding of α-actinin to GpIb-IX. The association between α-actinin and GpIb-IX is a direct consequence of VWF binding to GpIbα. VWF binding to GpIbα induces α-actinin binding to GpIb-IX through the stimulation of biochemical responses that result in larger amounts of filamentous actin cross-linked by α-actinin to bind to filamin A bound to the cytoplasmic domain of GpIbα.

Blocking VWF binding to αIIbβ3 has no effect on the association that develops between α-actinin and GpIb-IX in response to pathological shear stress. This occurs despite the fact that αIIbβ3 blockers inhibit several shear-induced platelet responses, including aggregation (*3*, *4*), an elevated level of cytosolic ionized calcium (*7*), pleckstrin phosphorylation (*8*), the tyrosine phosphorylation of many substrates (*9*, *10*), and, as demonstrated in Figure 4, the disassociation of α-actinin from integrin αIIbβ3. These results provide additional evidence that shear-induced VWF binding to platelet GpIbα initiates platelet activation but, for full platelet activation in response to pathological shearing stresses, VWF binding to both GpIb-IX and αIIbβ3 is required (*7*−*12*). They also present an analogy between platelets and rat fibroblasts which suggests a mechanism by which α-actinin binding to the β3 cytoplasmic domain in resting platelets could participate in platelet activation in response to shear stress. With data similar to those presented in Figure 4A showing that shear causes α-actinin to disassociate from β3, others have observed that α-actinin disassociates from the β3 tail of α$v\beta$3 when rat fibroblasts are stimulated by platelet-derived growth factor (*32*). This disassociation is directed by PI 3-K-generated phosphatidylinositol 3,4,5-trisphosphate, and it results in the "restructuring" of focal adhesions that allow for cell motility. Data presented in Figure 4 raise the possibility that an analogous response could occur as a consequence of VWF binding to αIIbβ3. Further studies should determine if functionally important shear-

induced αIIbβ3-mediated "outside-in signaling" occurs in platelets.

The data presented here also provide a clue to another biological response directed by α-actinin in sheared platelets. α-Actinin forms antiparallel homodimeric rods with actin binding domains at each end of the molecule (*33*). α-Actinin cross-linking filamentous actin provides the membrane skeleton with the mechanical property termed "strain hardening", which occurs when increasing elasticity results from a greater level of deformation. Strain hardening is believed to be one mechanism by which a mechanical force, including shear stress, is converted into cellular responses (*34*). Our data indicate that, in resting platelets, GpIb-IX is attached to the cortical skeleton through filamin A, but that the attachment is relatively depleted of the elastic deformability provided by α-actinin cross-linking. Following shear, elastic deformability is increased as α-actinin cross-linked to actin moves to a GpIb-IX-based compartment. The increased elastic deformability of the cytoplasmic tether of the GpIb-IX complex bound to extracellular VWF would develop slowly in platelets subjected to prolonged shearing stresses, and once developed, it could be an important factor responsible for maintaining cohesive forces that support platelet aggregation in the face of shearing stresses that disrupt almost all other cellular and protein interactions (*31*). It may also be one mechanism by which "inside-out" signaling to GpIb-IX appears to enhance the avidity of GpIbα for solid-phase VWF and maintain cell tethering in the face of shearing forces that prevent the attachment of leukocytes and the deposition of insoluble fibrin (*13*−*15*).

The functional importance of α-actinin phosphorylation is unknown. Because tyrosine phosphorylation occurs in the domain mediating actin binding (*23*), it could direct the actin cross-linking function of α-actinin. Data in Figure 7 showing that piceatannol inhibits α-actinin−GpIb-IX interactions are consistent with this. Such data are also consistent with the interpretation that an upstream tyrosine kinase (or kinases) signals two separate divergent responses, one of which is the phosphorylation of α-actinin and the other of which is the reorganization of the actin−α-actinin network resulting in its association with GpIb-IX.

Tyrosine-phosphorylated α-actinin could also serve to regulate signal molecule compartmentalization, including the assembly or disassembly of molecular complexes that include PI 3-K and PKN. Such compartmentalization probably is not related to binding SH2 domains in proteins, however, as sequence analysis of α-actinin does not reveal any ideal SH2 domain recognition motifs surrounding its phosphotyrosine residues (*23*, *35*). While there is evidence that the regulatory domain of class 1A heterodimeric PI 3-K, which contains two SH2 domains, binds directly to α-actinin (*21*), the tyrosine phosphorylation of α-actinin is unlikely to regulate its binding to PI 3-K in sheared platelets. This is because PI 3-K actually disassociates from α-actinin during the time period that α-actinin becomes phosphorylated. In fact, data in Figure 8 imply that the tyrosine phosphorylation of α-actinin could direct the disassociation of PI 3-K from α-actinin. Figure 8 also shows that the tyrosine phosphorylation of α-actinin could regulate its association with PKN. Like PI 3-K, however, PKN probably does not bind directly to a phosphopeptide recognition domain, since binding to PKN is through α-actinin's third spectrin-like repeat, which appears to remain unphosphorylated in activated platelets (*22*, *23*).

In conclusion, we have provided evidence that pathological shear stress-induced VWF binding to GpIb-IX triggers the translocation of tyrosine-phosphorylated α-actinin to GpIb-IX. This translocation results from cytoskeletal reorganization regulated by tyrosine kinases, and it may result in the assembly of a proaggregatory signaling complex associated with the cytoplasmic tail of GpIbα. α-Actinin binding to GpIb-IX may also result in alterations in the mechanical properties of the GpIb-IX complex bound to VWF that support platelet aggregation under high-shear conditions. Several critical questions remain, one being, "does tyrosine phosphorylation regulate α-actinin-mediated actin cross-linking or influence how α-actinin works as an adapter protein?" Answers to these questions should provide important insight into mechanisms of cellular activation generally, and could bring us closer to the development of antithrombotics that selectively inhibit pathways of platelet thrombus formation triggered only under conditions of pathologically elevated arterial wall shear stress.

ACKNOWLEDGMENT

We thank Dr. Richard Cook for his careful protein analyses and Dr. Perumal Thiagarajan for the rabbit anti-β3 polyclonal antibody.

REFERENCES

1. Baumgartner, H. R., Tschopp, T. B., and Meyer, D. (1980) *Br. J. Haematol. 44*, 127−139.
2. Turitto, V. T., Weiss, H. J., Zimmerman, T. S., and Sussman, I. I. (1985) *Blood 65*, 823−831.
3. Kroll, M. H., Hellums, J. D., McIntire, L. V., Schafer, A. I., and Moake, J. L. (1996) *Blood 88*, 1525−1541.
4. Savage, B., Almus-Jacobs, F., and Ruggeri, Z. M. (1998) *Cell 94*, 657−666.
5. Wu, Y.-P., Vink, T., Schiphorst, M., van Zanten, H., Ijsseldijk, J. W., de Groot, P. G., and Sixma, J. J. (2000) *Arterioscler. Thromb. Vasc. Biol. 20*, 1661−1667.
6. De Marco, L., Girolami, A., Zimmerman, T. S., and Ruggeri, Z. M. (1985) *Proc. Natl. Acad. Sci. U.S.A. 82*, 7424−7428.
7. Chow, T. W., Hellums, J. D., Moake, J. L., and Kroll, M. H. (1992) *Blood 80*, 113−120.
8. Kroll, M. H., Hellums, J. D., Guo, Z., Durante, W., Razdan, K., Hrbolich, J. K., and Schafer, A. I. (1993) *J. Biol. Chem. 268*, 3520−3524.
9. Razdan, K., Hellums, J. D., and Kroll, M. H. (1994) *Biochem. J. 302*, 681−686.
10. Oda, A., Yokoyama, K., Murata, M., Tokuhira, M., Nakamura, K., Handa, M., Watanabe, K., and Ikeda, Y. (1995) *Thromb. Haemostasis 74*, 736−742.
11. Goto, S., Salomon, D. R., Ikeda, Y., and Ruggeri, Z. M. (1995) *J. Biol. Chem. 270*, 23352−23361.
12. Polanowska-Grabowska, R., and Gear, A. (1999) *Arterioscler. Thromb. Vasc. Biol. 19*, 3044−3054.
13. Nemerson, Y., and Turitto, V. T. (1991) *Thromb. Haemostasis 66*, 272−276.
14. López, J. A. (1994) *Blood Coagulation Fibrinolysis 5*, 97−119.
15. Feng, S., Christodoulides, N., Resendiz, J. C., Berndt, M. C., and Kroll, M. H. (2000) *Blood 95*, 551−557.
16. Andrews, R. K., and Fox, J. E. (1992) *J. Biol. Chem. 267*, 18605−18611.
17. Cunningham, J. G., Meyer, S. C., and Fox, J. E. B. (1996) *J. Biol. Chem. 271*, 11581−11587.
18. Du, X., Fox, J. E., and Pei, S. (1996) *J. Biol. Chem. 271*, 7362−7367.

19. Feng, S., Christodoulides, N., and Kroll, M. H. (1999) *Blood 93*, 4256−4263.
20. Gu, M., Xi, X., Englund, G. D., Berndt, M. C., and Du, X. (1999) *J. Cell Biol. 147*, 1085−1096.
21. Shibasaki, F., Fukami, K., Fuku, Y., and Takenawa, T. (1994) *Biochem. J. 302*, 551−557.
22. Mukai, H., Toshimori, M., Shibata, H., Takanaga, H., Kitagawa, M., Miyahara, M., Shimakawa, M., and Ono, Y. (1997) *J. Biol. Chem. 272*, 4740−4746.
23. Izaguirre, G., Aguirre, L., Hu, Y.-P., Lee, H. Y., Schlaepfer, D. D., Aneskievich, B. J., and Haimovich, B. (2001) *J. Biol. Chem. 276*, 28676−28685.
24. Izaguirre, G., Aguirre, L., Ji, P., Aneskievich, B., and Haimovich, B. (1999) *J. Biol. Chem. 274*, 37012−37020.
25. Hoffmeister, K. M., Falet, H., Toker, A., Barkalow, K. L., Stossel, T. P., and Hartwig, J. H. (2001) *J. Biol. Chem. 276*, 24751−24759.
26. Calderwood, D. A., Shattil, S. J., and Ginsberg, M. H. (2000) *J. Biol. Chem. 275*, 22607−22610.
27. Law, D., Nanizzi-Alaimo, L., Ministri, K., Hughes, P. E., Forsyth, J., Turner, M., Shattil, S. J., Ginsberg, M. H., Tybulewicz, V. L. J., and Phillips, D. R. (1999) *Blood 93*, 2645−2652.
28. Kroll, M. H., Harris, T. S., Moake, J. L., Handin, R. I., and Schafer, A. I. (1991) *J. Clin. Invest. 88*, 1568−1573.
29. Jackson, S. P., Schoenwaelder, S. M., Yuan, Y., Rabinowitz, I., Salem, H. H., and Mitchell, C. A. (1994) *J. Biol. Chem. 269*, 27093−27099.
30. Reséndiz, J. C., Feng, S., Christodoulides, N. C., Arboleda, D., Berndt, M. C., and Kroll, M. H. (2000) *Blood 96*, 1045a.
31. Christodoulides, N. C., Feng, S., Reséndiz, J. C., Berndt, M. C., and Kroll, M. H. (2001) *Thromb. Res. 102*, 133−142.
32. Greenwood, J. A., Thiebert, A. B., Prestwich, G. D., and Murphy-Ullrich, J. E. (2000) *J. Cell Biol. 150*, 627−641.
33. Djinoviæ-Carugo, K., Young, P., Gautel, M., and Saraste, M. (1999) *Cell 98*, 537−546.
34. Xu, J., Tseng, Y., and Wirtz, D. (2000) *J. Biol. Chem. 275*, 35886−35892.
35. Songyang, Z., et al. (1993) *Cell 72*, 767−778.

BI0156005